

## Pyridine substituted BODIPYs: synthesis, characterization and cholinesterase, $\alpha$ -glucosidase inhibitory, DNA hydrolytic cleavage effects

Burak BARUT<sup>1</sup> , Hüseyin BAŞ<sup>2</sup> , Zekeriya BIYIKLIOĞLU<sup>2,\*</sup> 

<sup>1</sup>Department of Biochemistry, Karadeniz Technical University, Trabzon, Turkey

<sup>2</sup>Department of Chemistry, Karadeniz Technical University, Trabzon, Turkey

Received: 26.05.2021 • Accepted/Published Online: 09.07.2021 • Final Version: 19.10.2021

**Abstract:** In this study, the synthesis of new monostyryl (BDPY-2) and distyryl BODIPY dyes (BDPY-4, BDPY-5) containing pyridine groups has been reported for the first time. The acetylcholinesterase from *Electrophorus electricus* (AChE), butyrylcholinesterase from equine serum (BuChE),  $\alpha$ -glucosidase from *Saccharomyces cerevisiae* and DNA hydrolytic cleavage actions of BDPY-2, BDPY-4, BDPY-5 were investigated using various techniques. The results indicated that the compounds had varying inhibition properties against AChE, BuChE, and  $\alpha$ -glucosidase. BDPY-4 was the most potent compound on AChE with  $IC_{50}$  of  $54.78 \pm 4.51 \mu\text{M}$ , and Lineweaver-Burk plots indicated that the compound is bound to a site other than the active site as a noncompetitive inhibitor. The compound-protein binding experiment showed that BDPY-4 changed the microenvironment around AChE. On the other hand, the compounds showed lower  $\alpha$ -glucosidase inhibition than the positive control. The DNA hydrolytic cleavage effects were not observed on supercoiled plasmid DNA in the presence of the compounds as compared to negative controls. These findings suggested that BDPY-4 might be a promising compound to treat Alzheimer's diseases.

**Key words:** Synthesis, BODIPY, anticholinesterase, DNA hydrolytic cleavage

### 1. Introduction

Alzheimer's disease (AD) is one of the major global health challenges among the elderly population and a chronic and progressive syndrome categorized by developing memory and perception impairment [1,2]. Nowadays, nearly 50 million people are affected by this illness worldwide, and there will be more than 120 million new cases estimated in 2050 [3,4]. The etiology of AD involves many pathways including low acetylcholine level, overproduction of the beta-amyloid peptide, hypoxia, reactive oxygen species, and tau protein phosphorylation [5]. Up till now, an effective therapeutic strategy is to boost acetylcholine levels in the brain by inhibiting cholinesterase enzymes (acetylcholinesterase (AChE), butyrylcholinesterase (BuChE)) and regulate acetylcholine in the human body [6]. To date, very few inhibitors are approved few drugs for AD treatment by the United States Food and Drug Administration (FDA) such as tacrine, galantamine, donepezil, but they impart several adverse effects such as hepatotoxicity, gastrointestinal disorders, and periphery side effects [5,7].

Diabetes mellitus (DM) is a chronic metabolic disorder caused by hyperglycemia with less insulin action or secretion or both [8]. DM triggers severe health complications including neuropathy, nephropathy, cancer, retinopathy, etc. Thus, the most effective strategy of DM treatment is to regulate bloodstream glucose levels control [9].  $\alpha$ -Glucosidase inhibitors have important roles to decrease glucose levels in the bloodstream by preventing the breakdown of carbohydrates into absorbable monosaccharides [10]. However,  $\alpha$ -glucosidase inhibitors have several side effects such as gastrointestinal disorders, etc. [11]. Thus, it is crucial to seek for low side effect profile  $\alpha$ -glucosidase inhibitors.

4,4-Difluoro-4-bora-3a,4a-diaza-s-indacene (BODIPY), developed by Treibs and Kreuzer in 1968, displays a wide range of research fields such as material, medical research, diagnosis, and treatment due to their strong absorption, high fluorescence quantum efficiency, and stable chemical structure properties [12–14]. They have been used for variety of applications *viz.* as laser dyes, drug delivery, solar cells, fluorescent labels, anticancer agents in photodynamic therapy [15–22].

In medicinal chemistry, pyridine is a versatile heterocyclic nucleus finding applications. It is well-known that they have been exhibited various pharmacological and biological activities such as antiviral, anticancer, antidiabetic, anticonvulsant,

\* Correspondence: zekeriyaab@ktu.edu.tr

anticholinesterase, antimicrobial, antiinflammatory, etc. [23–29]. Here, we aimed to define the biological activity of the **BDPY-2**, **BDPY-4**, and **BDPY-5** compounds on AChE, BuChE,  $\alpha$ -glucosidase, and DNA.

## 2. Experimental

The materials, equipment, AChE, BuChE,  $\alpha$ -glucosidase inhibitory, and DNA hydrolytic cleavage actions are given as supplementary information.

### 2.1. Synthesis

#### 2.1.1. 4-(3-Pyridin-4-ylpropoxy)benzaldehyde (1)

4-hydroxybenzaldehyde (1.57 g, 12.8 mmol),  $K_2CO_3$  (3.53 g, 25.6 mmol), pyridine derivative (2 g, 12.8 mmol) were mixed in 20 mL dry DMF under nitrogen at 85 °C for 24 h. The mixture was poured into ice-water and added 100 mL chloroform. Organic phase was dried with  $Na_2SO_4$ , and the crude product was performed to chromatograph on an aluminum oxide with chloroform as an eluent. Yield: 2.01 g (65%). IR (ATR),  $\nu/cm^{-1}$ : 3075 (Ar-H), 2955–2877 (Aliph. C-H), 1671 (C=O), 1592, 1507, 1469, 1425, 1397, 1311, 1255, 1214, 1151, 1110, 1018, 885, 799, 614.  $^1H$  NMR (400 MHz, DMSO- $d_6$ ), ( $\delta$ ): 9.87 (s, 1H, =CH), 8.47 (d, 2H, ArH), 7.87 (d, 2H, ArH), 7.29 (d, 2H, ArH), 7.12 (d, 2H, ArH), 4.10 (t, 2H,  $CH_2-O$ ), 2.78 (t, 2H, Ar- $CH_2$ ), 2.10-2.06 (m, 2H,  $-CH_2-$ ).  $^{13}C$ -NMR (DMSO- $d_6$ ), ( $\delta$ ): 191.76, 163.96, 150.93, 149.80, 132.29, 130.10, 124.46, 115.38, 67.68, 31.15, 29.39. MALDI-TOF-MS  $m/z$ : 241.46 [M] $^+$ .

#### 2.1.2. BODIPY-2 (BDPY-2)

Compound (1) (250 mg, 1.04 mmol), 2,4-dimethylpyrrole (0.23 mL, 2.08 mmol) and four drop of trifluoroacetic acid (TFA) were dissolved in dichloromethane (200 mL) stirred at rt for 24h. Then a solution of 2,3-dichloro-5,6-dicyano-1,4-benzoquinone (DDQ) (237 mg, 1.04 mmol) in  $CH_2Cl_2$  (5 mL) was added slowly to the mixture. 3 mL triethyl amine ( $NEt_3$ ) was added. Then, 3 mL boron trifluoride diethyl etherate ( $BF_3 \cdot OEt_2$ ) was added, and the reaction mixture stirred for 24h at rt. The mixture was washed with water, and the organic phase was dried over  $MgSO_4$ ; the solvent was evaporated under reduced pressure. The product was performed to chromatographed on an aluminum oxide column with a  $CH_2Cl_2$ :hexane (4:1) as solvent system. Yield: 261 mg (55%). IR (ATR)  $\nu$  ( $cm^{-1}$ ): 3072 (Ar-H), 2923-2864 (Aliph. C-H), 1603, 1542, 1506, 1467, 1410, 1367, 1304, 1241, 1190, 1155, 1074, 972, 795.  $^1H$ -NMR (400 MHz, DMSO- $d_6$ ), ( $\delta$ ): 8.45 (m, 2H, ArH), 7.28-7.25 (m, 2H, ArH), 7.10 (d, 2H, ArH), 6.89 (d, 2H, ArH), 6.17 (s, 2H, =CH), 4.04 (t, 2H,  $CH_2-O$ ), 3.91 (t, 2H, Ar- $CH_2-$ ), 2.44 (s, 6H,  $CH_3$ ), 2.02-1.99 (m, 2H,  $-CH_2-$ ), 1.39 (s, 6H,  $CH_3$ ).  $^{13}C$ -NMR (DMSO- $d_6$ ), ( $\delta$ ): 155.11, 150.83, 149.94, 143.20, 142.60, 136.32, 131.56, 129.57, 127.14, 124.41, 121.74, 115.65, 67.28, 66.97, 31.22, 29.54, 14.60. UV-Vis ( $CHCl_3$ )  $\lambda_{max}$  nm (log  $\epsilon$ ): 503 (4.99). MALDI-TOF-MS  $m/z$ : 459.70 [M+H] $^+$ .

#### 2.1.3. BODIPY-4 (BDPY-4)

BODIPY 2 (100 mg, 0.21 mmol) and compound (1) (131 mg, 0.54 mmol) were dissolved in toluene (25 mL). Glacial acetic acid (0.3 mL, 3.57 mmol), piperidine (0.3 mL, 2.61 mmol), and a catalytic amount of magnesium perchlorate were added. The mixture was refluxed using Dean-Stark trap apparatus until was residuum. The product was performed to chromatographed on an aluminum oxide column with a  $CHCl_3$ :benzene (3:2) as solvent system. Yield: 57 mg (30%). IR (ATR)  $\nu$  ( $cm^{-1}$ ): 3067 (Ar-H), 2918–2849 (Aliph. C-H), 1597, 1537, 1509, 1485, 1461, 1385, 1242, 1199, 1161, 1107, 989, 823.  $^1H$  NMR (400 MHz, DMSO- $d_6$ ), ( $\delta$ ): 8.51-8.46 (m, 8H, ArH), 7.58 (d, 4H, ArH), 7.40-7.36 (m, 8H, ArH), 7.13 (d, 4H, ArH), 7.04 (d, 2H, ArH), 6.94 (s, 2H, =CH), 6.82 (d, 2H, Ar-H), 4.07 (t, 6H,  $CH_2-O$ ), 2.89-2.84 (m, 6H, Ar- $CH_2$ ), 2.14-2.11 (m- 6H,  $-CH_2-$ ), 1.47 (s, 6H,  $CH_3$ ).  $^{13}C$  NMR (DMSO- $d_6$ ), ( $\delta$ ): 160.27, 160.03, 157.38, 155.31, 155.23, 155.07, 148.81, 147.62, 147.39, 147.16, 137.23, 137.12, 137.01, 136.94, 136.76, 130.11, 129.32, 129.06, 124.86, 115.62, 114.99, 67.30, 66.96, 31.37, 15.85. UV-Vis ( $CHCl_3$ )  $\lambda_{max}$  nm (log  $\epsilon$ ): 644 (5.01), 591 (4.63), 370 (4.83). MALDI-TOF-MS  $m/z$ : 905.79 [M] $^+$ .

#### 2.1.4. BODIPY-5 (BDPY-5)

**BODIPY 5** was synthesized similarly to **BODIPY-4** by using compound (3) instead of compound (1). The product was purified by aluminum oxide column chromatography using chloroform as solvent. Yield: 123 mg (65%). IR (ATR)  $\nu$  ( $cm^{-1}$ ): 3029 (Ar-H), 2919–2850 (Aliph. C-H), 1599, 1537, 1509, 1486, 1422, 1386, 1295, 1242, 1162, 1140, 1106, 1025, 990, 939, 826, 711.  $^1H$  NMR (400 MHz, DMSO- $d_6$ ), ( $\delta$ ): 8.44-8.39 (m, 8H, ArH), 7.65 (d, 4H, ArH), 7.43 (s, 2H, ArH), 7.31-7.28 (m, 4H, ArH), 7.12 (d, 8H, ArH), 6.93 (s, 2H, =CH), 6.82 (d, 2H, ArH), 3.90 (t, 6H,  $CH_2-O$ ), 2.73 (t, 6H, Ar- $CH_2$ ), 2.01-1.97 (m- 6H,  $-CH_2-$ ), 1.45 (s, 6H,  $CH_3$ ).  $^{13}C$  NMR (DMSO- $d_6$ ), ( $\delta$ ): 160.11, 157.43, 152.48, 149.90, 147.63, 142.00, 138.72, 137.36, 136.97, 136.38, 133.32, 132.87, 130.08, 129.30, 126.65, 124.44, 123.95, 118.47, 116.39, 115.59, 114.98, 67.28, 66.93, 30.46, 14.85. UV-Vis ( $CHCl_3$ )  $\lambda_{max}$  nm (log  $\epsilon$ ): 646 (5.04), 593 (4.62), 372 (4.86). MALDI-TOF-MS  $m/z$ : 906.00 [M+H] $^+$ .

### 3. Results and discussion

#### 3.1. Synthesis and characterization

The synthesis of monostyryl (BDPY-2), distyryl BODIPY dyes (BDPY-4, BDPY-5) containing pyridine groups are presented in Figure 1. Compound (1) was synthesized from the reaction of 4-(3-chloropropyl)pyridine with 4-hydroxybenzaldehyde in DMF. The monostyryl BDPY-2 was prepared by treating 2,4-dimethylpyrrole with 4-(3-pyridin-4-ylpropoxy)benzaldehyde in the presence of TFA, DDQ,  $\text{NEt}_3$ ,  $\text{BF}_3 \cdot \text{OEt}_2$  in  $\text{CH}_2\text{Cl}_2$ . Then, distyryl BODIPY dyes (BDPY-4, BDPY-5)

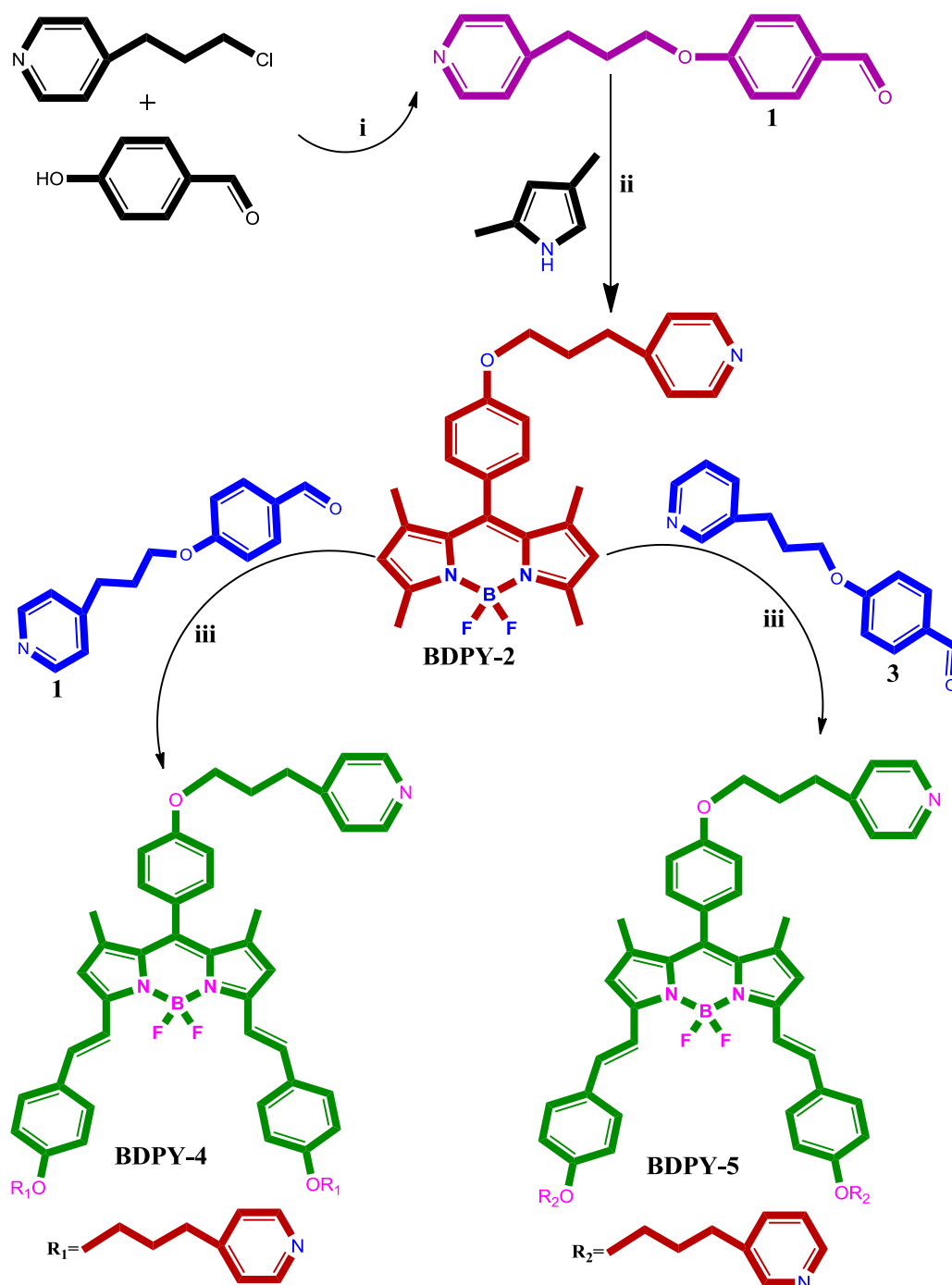


**Figure 1.** The synthesis of BODIPY dyes 2, 4 and 5. (i)  $\text{K}_2\text{CO}_3$ , 85 °C, DMF. (ii) 2,4-dimethylpyrrole, DCM, TFA, DDQ,  $\text{NEt}_3$ ,  $\text{BF}_3 \cdot \text{OEt}_2$ . (iii) Glacial acetic acid, piperidine,  $\text{Mg}(\text{ClO}_4)_2$ , toluene.

were synthesized using monostyryl **BDPY-2**, compound (1), compound (3) [20], piperidine,  $\text{Mg}(\text{ClO}_4)_2$  as a catalyst in toluene at reflux temperature.

In the IR spectrum of (1),  $-\text{C}=\text{O}$  peak of (1) seemed at  $1671\text{ cm}^{-1}$ . In the  $^1\text{H-NMR}$  spectrum of (1), the aldehyde proton ( $=\text{CH}$ ) resonated at  $9.87\text{ ppm}$ . In the  $^{13}\text{C-NMR}$  spectrum of (1), the  $\text{C}=\text{O}$  group appeared at  $191.76\text{ ppm}$ . The molecular ion peak of (1) was shown as  $241.46\text{ [M]}^+$ . In the IR spectrum of monostyryl **BDPY-2**, aldehyde peaks of (1) disappeared. In the  $^1\text{H-NMR}$  spectrum of monostyryl **BDPY-2**, aldehyde proton ( $=\text{CH}$ ) vanished, and pyrrole  $=\text{CH}$  protons appeared at  $6.17\text{ ppm}$ . The  $^{13}\text{C-NMR}$  data of **BDPY-2** confirmed the structure. In the MALDI-TOF-MS of **BDPY-2**, the presence of the molecular ion peak at  $m/z = 459.70\text{ [M+H]}^+$  confirmed the structure. The IR spectra of distyryl BODIPY dyes (**BDPY-4**, **BDPY-5**) were similar with **BDPY-2**. In the  $^1\text{H-NMR}$  spectra of **BDPY-4**, **BDPY-5**, pyrrole  $=\text{CH}$  was observed at  $6.94\text{ ppm}$  for **BDPY-4**,  $6.93\text{ ppm}$  for **BDPY-5**. Also, The  $^{13}\text{C-NMR}$  data of **BDPY-4** and **BDPY-5** confirmed the structures. The molecular ion peaks were observed at  $m/z: 905.79$  as  $[\text{M}]^+$  for **BDPY-4** (Figure S1a),  $906.00$  as  $[\text{M+H}]^+$  for **BDPY-4** (Figure S1b). The UV-Vis spectra of **BDPY-2**, **BDPY-4**, **BDPY-5** were recorded in  $\text{CHCl}_3$  (Figure 2). As shown in Figure 3, **BDPY-**

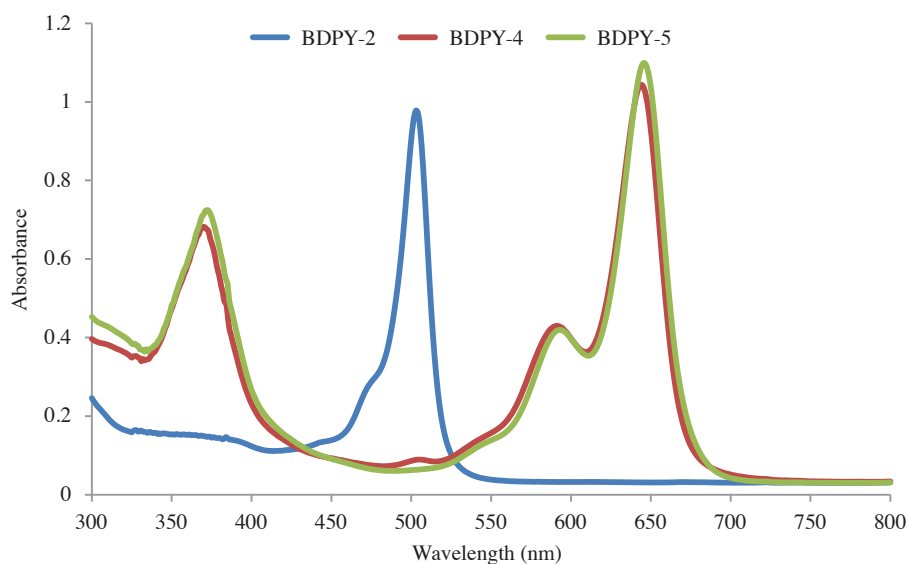


Figure 2. UV-Vis spectra of **BDPY-2**, **BDPY-4**, **BDPY-5** in  $\text{CHCl}_3$ .

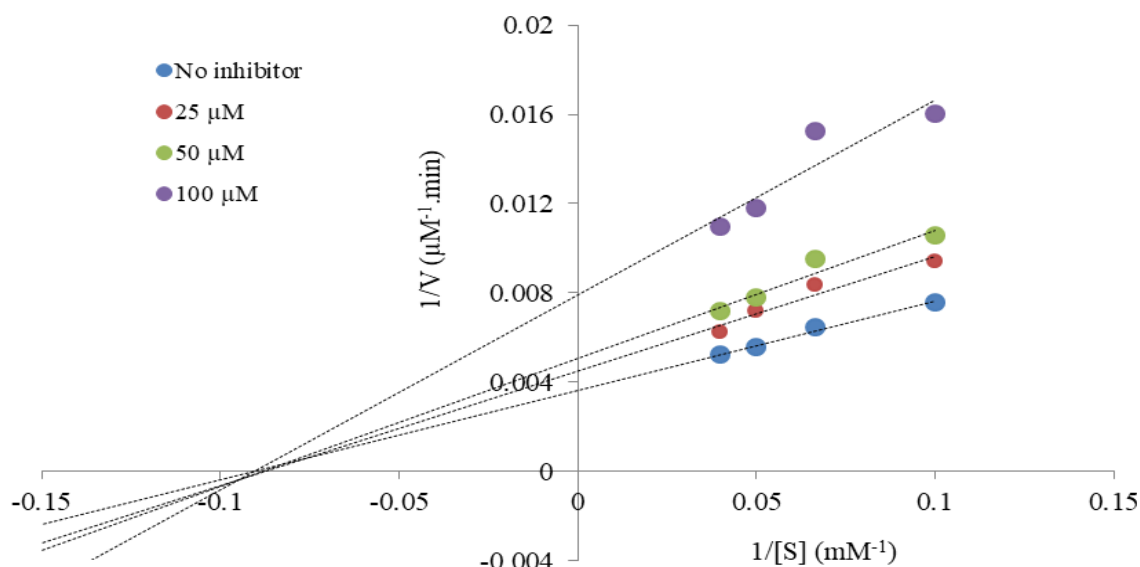


Figure 3. Lineweaver-Burk plot of **BDPY-4** on AChE.

2 showed an absorption peak at 503 nm, which is based on a  $S_0 \rightarrow S_1$  ( $\pi-\pi^*$ ) transition. Introduction of compound (1), compound (3) to the BDPY-2 to give BDPY-4, BDPY-5 lead to red shifts (141 nm and 143 nm) in both the absorptions. BDPY-4 and BDPY-5 indicated absorption peaks at 644 nm and 646 nm.

### 3.2. AChE/BuChE inhibitory properties of the compounds

The inhibition actions of the compounds (BDPY-2, BDPY-4, and BDPY-5) on AChE and BuChE were investigated according to our previously reported methods [30]. The results were expressed as  $IC_{50}$  and selective index (SI=BuChE/AChE) values. As shown in Table 1, the compounds showed dose-dependent inhibition on AChE and BuChE and  $IC_{50}$  values of the compounds ranged from  $54.78 \pm 4.51$  to  $184.87 \pm 5.49$   $\mu\text{M}$ . BDPY-4 was the most potent compound on AChE with an  $IC_{50}$  of  $54.78 \pm 4.51$   $\mu\text{M}$ . The  $IC_{50}$  values of BDPY-2 and BDPY-5 were determined as  $72.46 \pm 2.95$  and  $64.89 \pm 3.89$   $\mu\text{M}$ , respectively against AChE. On the other hand, the  $IC_{50}$  values of BDPY-2, BDPY-4, and BDPY-5 were  $184.87 \pm 5.49$ ,  $150.30 \pm 6.09$ , and  $170.30 \pm 4.33$   $\mu\text{M}$ , respectively on BuChE. The SI values of BDPY-2, BDPY-4, and BDPY-5 were 2.55, 2.74, and 2.62. The results showed that the compounds had lower anticholinesterase effects than galantamine as a positive control ( $IC_{50}$ :  $36.25 \pm 0.58$   $\mu\text{M}$  for AChE;  $65.32 \pm 0.99$   $\mu\text{M}$  for BuChE), but they have a higher selective index (SI<sub>galantamine</sub>: 1.80).

The mechanism for AChE inhibition was graphically determined by applying the Lineweaver–Burk and Dixon plots analysis of the most potent compound (BDPY-4). Acetylthiocholine iodide was used as a substrate for AChE inhibition. Lineweaver–Burk plot showed that  $K_m$  (an index of the affinity of the enzyme for its substrate) was in similar values, but  $V_{max}$  (maximal velocity of the reaction) decreased on increasing concentrations of the compound on AChE. While the  $K_m$  value was 11.14 mM, the  $V_{max}$  values changed from 277.78  $\mu\text{M}/\text{min}$  to 126.58  $\mu\text{M}/\text{min}$  (Figure 3, Table 2). The results indicated that BDPY-4 was a noncompetitive inhibitor and bound to a site other than the active site. On the other hand, BDPY-4 presented  $K_i$  (inhibition constant) values of  $57.20 \pm 0.20$   $\mu\text{M}$ , according to the Dixon plot (Figure 4, Table 3).

To determine the structural change of AChE (10  $\mu\text{M}$ ) induced by BDPY-4, we measured the UV-Vis spectroscopy by adding the compound (5, 10, 15, and 20  $\mu\text{M}$ ) into AChE solution (10  $\mu\text{M}$ ). AChE has an absorption peak at 282 nm due to aromatic amino acids. As shown in Figure 5, the absorbance of the enzyme increased with various BDPY-4 concentrations (hyperchromism). In addition, the absorption peak shifted from 282 nm to 285 nm (redshift). The UV-Vis spectrum implies that BDPY-4 showed binding with enzyme and changed the microenvironment of some amino acid residues of AChE.

### 3.3. $\alpha$ -Glucosidase inhibitory properties of the compounds

The inhibitory properties of the compounds on  $\alpha$ -glucosidase were investigated according to our previously reported methods [31]. The results were expressed as  $IC_{50}$  values. As shown in Table 4,  $IC_{50}$  values of the compounds ranged from  $94.99 \pm 4.77$  to  $218.62 \pm 8.71$   $\mu\text{M}$ . BDPY-4 was the highest  $\alpha$ -glucosidase inhibitory effects among the tested compounds, but the compound showed lower inhibitory than acarbose used as a positive control ( $IC_{50}$ = $32.22 \pm 0.40$   $\mu\text{M}$ ).

**Table 1.** The  $IC_{50}$  ( $\mu\text{M}$ ) and SI (BuChE/AChE) values of the compounds on AChE and BuChE.

	AChE	BuChE	SI
<b>BDPY-2</b>	$72.46 \pm 2.95$	$184.87 \pm 5.49$	2.55
<b>BDPY-4</b>	$54.78 \pm 4.51$	$150.30 \pm 6.09$	2.74
<b>BDPY-5</b>	$64.89 \pm 3.89$	$170.30 \pm 4.33$	2.62
<b>Galantamine</b>	$36.25 \pm 0.58$	$65.32 \pm 0.99$	1.80

**Table 2.** The  $V_{max}$  and  $K_m$  values of the BDPY-4 on AChE.

	$V_{max}$	$K_m$
<b>No inhibitor</b>	277.78 $\mu\text{M}/\text{min}$	11.14 mM
<b>25 <math>\mu\text{M}</math></b>	222.22 $\mu\text{M}/\text{min}$	11.14 mM
<b>50 <math>\mu\text{M}</math></b>	196.08 $\mu\text{M}/\text{min}$	11.14 mM
<b>100 <math>\mu\text{M}</math></b>	126.58 $\mu\text{M}/\text{min}$	11.14 mM

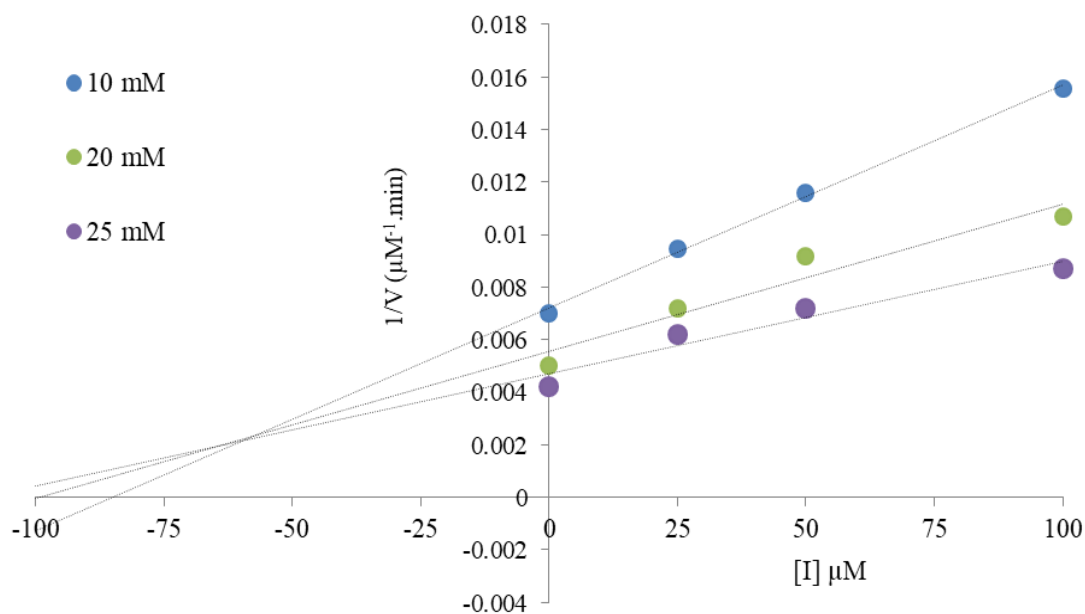


Figure 4. Dixon plot of BDPY-4 on AChE.

Table 3. The inhibitory type and  $K_i$  value of the BDPY-4 on AChE.

	Type	$K_i$
BDPY-4	noncompetitive	$57.20 \pm 0.20 \mu\text{M}$

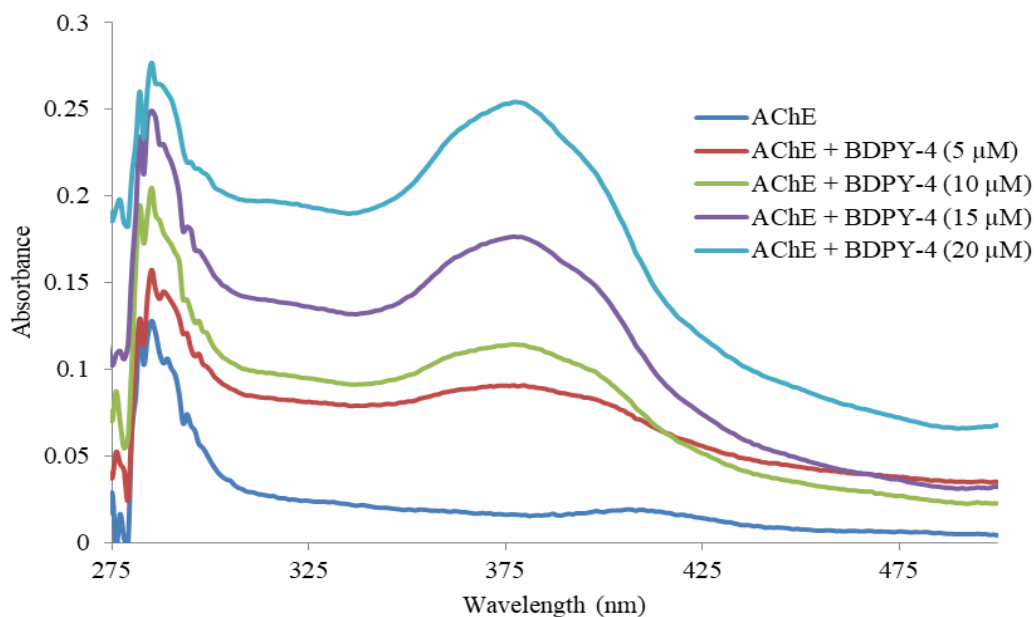


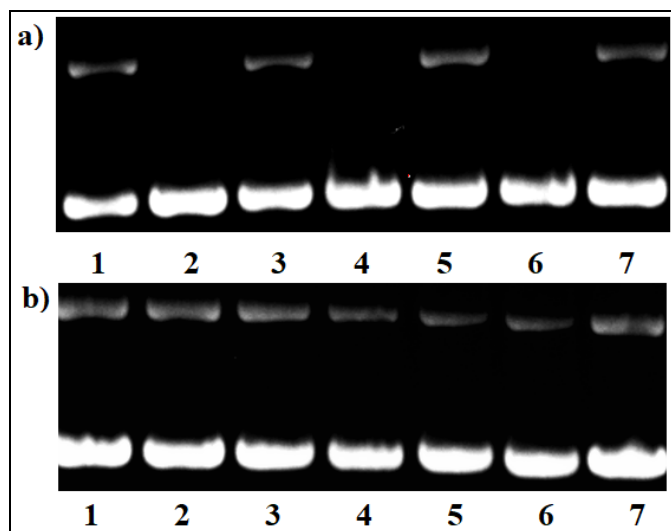
Figure 5. UV-Vis spectrum of BDPY-4-AChE complexes.

### 3.4. DNA hydrolytic cleavage properties of the compounds

The DNA hydrolytic cleavage actions of the compounds on supercoiled pBR322 plasmid DNA were determined according to our previously reported methods, and the intensity bands were observed under UV illuminator [32]. To investigate the ability of the compounds to damage the phosphodiester bonds of supercoiled plasmid DNA, we designed hydrolytic

**Table 4.** The IC<sub>50</sub> (μM) values of the compounds on α-glucosidase.

	α-glucosidase
<b>BDPY-2</b>	218.62 ± 8.71
<b>BDPY-4</b>	94.99 ± 4.77
<b>BDPY-5</b>	105.83 ± 5.03
<b>Acarbose</b>	32.22 ± 0.40

**Figure 6.** DNA hydrolytic nuclease effects of the compounds for 30 min (a), 60 min (b). Lane 1: DNA control; lanes 2–3: 25 and 50 μM of (BDPY-2); lanes 4–5: 25 and 50 μM of (BDPY-4); lanes 6–7: 25 and 50 μM of (BDPY-5).

cleavage studies. The supercoiled plasmid DNA has three forms in agarose gel: form I (supercoiled form), form II (nicked form cleavage of one strand), form III (linear form cleavage of two strands). The results are presented in Figure 6. It is known that supercoiled pBR322 plasmid DNA (Thermo Fischer Scientific, SD0041) is in the supercoiled form at a rate of more than 90%. Since the plasmid DNA has impurity, the density of Form II is increased on negative controls. In this study, the presence of the compounds did not have DNA hydrolytic cleavage effects at 25 and 50 μM as compared to negative controls (Figures 6(a),(b), lanes 1) under our experimental conditions. The results claimed that these compounds may have low toxicity potential in the dark as a preliminary study.

#### 4. Conclusion

In conclusion, we have synthesized new monostyryl (BDPY-2) and distyryl BODIPY dyes (BDPY-4, BDPY-5) and investigated their acetylcholinesterase from *Electrophorus electricus* (AChE), butyrylcholinesterase from equine serum (BuChE), α-glucosidase from *Saccharomyces cerevisiae*, and DNA hydrolytic cleavage actions. The compounds showed varying inhibition actions against AChE, BuChE, and α-glucosidase. BDPY-4, which was a noncompetitive inhibitor, was the most potent compound on AChE with an IC<sub>50</sub> of 54.78 ± 4.51 μM. The UV-vis spectroscopy studies claimed that it interacted with enzyme change the microenvironment around AChE. In addition, the compounds had low α-glucosidase inhibitory effects when compared to acarbose. The DNA hydrolytic cleavage was not showed on supercoiled plasmid DNA in the presence of the compounds at 25 and 50 μM as compared to negative controls under our experimental conditions. These findings suggested that these compounds have low toxicity potential in the dark. Further studies are needed regarding anticholinesterase and toxicity effects of BDPY-4 on development of formulations, cell cultures, and in vivo studies for application in internal diseases.

#### Acknowledgments

This study was not supported by any organization.

## References

1. Yan X, Chen T, Zhang L, Du H. Study of the interactions of forsythiaside and rutin with acetylcholinesterase (AChE). *International Journal of Biological Macromolecules* 2018; 119: 1344-1352.
2. Shaikh S, Pavale G, Dhavan P, Singh P, Uparkar J et al. Design, synthesis and evaluation of dihydropyranoindole derivatives as potential cholinesterase inhibitors against Alzheimer's disease. *Bioorganic Chemistry* 2021; 110: 104770.
3. World Health Organization (2021). Dementia [online]. Website <https://www.who.int/news-room/fact-sheets/detail/dementia> [accessed date: 01 May 2021].
4. Prince M, Wimo A, Guerchet M, Ali GC, Wu YT et al. Alzheimer's Disease International: World Alzheimer Report 2015. London, England: Alzheimer's Disease International (ADI), 2015.
5. Borioni JL, Cavallaro V, Murray AP, Peñeñory AB, Puiatti M et al. Design, synthesis and evaluation of cholinesterase hybrid inhibitors using a natural steroidal alkaloid as precursor. *Bioorganic Chemistry* 2021; 111: 104893.
6. Kumar RS, Almansour AI, Arumugam N, Kotresha D, Manohar TS et al. Cholinesterase inhibitory activity of highly functionalized fluorinated spiropyrrolidine heterocyclic hybrids. *Saudi Journal of Biological Sciences* 2021; 28: 754-761.
7. Barut B, Demirbaş Ü. Synthesis, anti-cholinesterase,  $\alpha$ -glucosidase inhibitory, antioxidant and DNA nuclease properties of non-peripheral triclosan substituted metal-free, copper(II), and nickel(II) phthalocyanines. *Journal of Organometallic Chemistry* 2020; 923: 121423.
8. Sherafati M, Mirzazadeh R, Barzegari E, Mohammadi-Khanaposhtani M, Azizian H et al. Quinazolinone-dihydropyrano[3,2-b]pyran hybrids as new  $\alpha$ -glucosidase inhibitors: Design, synthesis, enzymatic inhibition, docking study and prediction of pharmacokinetic. *Bioorganic Chemistry* 2021; 109: 104703.
9. Kasturi SP, Surarapu S, Uppalanchi S, Dwivedi S, Yogeewari P et al. Synthesis, molecular modeling and evaluation of  $\alpha$ -glucosidase inhibition activity of 3,4-dihydroxy piperidines. *European Journal of Medicinal Chemistry* 2018; 150: 39-52.
10. Mphahlele MJ, Magwaza NM, Gildenhuis S, Setschedi IB. Synthesis,  $\alpha$ -glucosidase inhibition and antioxidant activity of the 7-carbo-substituted 5-bromo-3-methylindazoles. *Bioorganic Chemistry* 2020; 97: 103702.
11. Kumar L, Lal K, Yadav P, Kumar A, Paul AK. Synthesis, characterization,  $\alpha$ -glucosidase inhibition and molecular modeling studies of some pyrazoline-1H-1,2,3-triazole hybrids. *Journal of Molecular Structure* 2020; 1216: 128253.
12. Lv Z, Wang Y, Zhang J, Wang Z, Jin G. Bis-sulfonyl-chalcone-BODIPY molecular probes for in vivo and in vitro imaging. *Journal of Molecular Structure* 2021; 1234: 130201.
13. Zhang W, Ahmed A, Cong H, Wang S, Shen Y et al. Application of multifunctional BODIPY in photodynamic therapy. *Dyes and Pigments* 2021; 185: 108937.
14. Treibs A, Kreuzer F. Difluoroboryl-Komplexe von Di- und Tripyrrylmethenen. *Justus Liebigs Annalen der Chemie* 1968; 718 208-223.
15. Duran-Sampedro G, Agarrabeitia AR, Garcia-Moreno I, Costela A, Bañuelos J et al. Chlorinated BODIPYs: Surprisingly efficient and highly photostable laser dyes. *European Journal of Organic Chemistry* 2012; 32: 6335-6350.
16. McCusker C, Carrol JB, Rotello VM. Cationic polyhedral oligomeric silsesquioxane (POSS) units as carriers for drug delivery processes. *Chemical Communications* 2005; 28: 996-998.
17. Kumaresan D, Thummel RP, Bura T, Ulrich G, Ziessel R. Color tuning in new metal-free organic sensitizers (Bodipys) for dye-sensitized solar cells. *Chemistry A European Journal*. 2009; 15: 6335-6339.
18. Monsma FJ, Barton AC, Kang HC, Brassard DL, Haugland RP et al. Characterization of novel fluorescent ligands with high affinity for D1 and D2 dopaminergic receptors. *Journal of Neurochemistry* 1989; 52: 1641-1644.
19. Barut B, Çoban Ö, Yalçın CÖ, Baş H, Sari S et al. Synthesis, DNA interaction, in vitro/in silico topoisomerase II inhibition and photodynamic therapy activities of two cationic BODIPY derivatives. *Dyes and Pigments* 2020; 174: 108072.
20. Barut B, Yalçın CÖ, Sari S, Çoban Ö, Keleş T et al. Novel water soluble BODIPY compounds: Synthesis, photochemical, DNA interaction, topoisomerases inhibition and photodynamic activity properties. *European Journal of Medicinal Chemistry* 2019; 183: 111685.
21. Turksoy A, Yildiz D, Akkaya EU. Photosensitization and controlled photosensitization with BODIPY dyes. *Coordination Chemistry Reviews* 2019; 379: 47-64.
22. Derin Y, Yılmaz RE, Baydilek İH, Atalay VE, Özdemir A et al. Synthesis, electrochemical/photophysical properties and computational investigation of 3,5-dialkyl BODIPY fluorophores. *Inorganica Chimica Acta* 2018; 482: 130-135.
23. Bernardino AMR, da Silva Pinheiro LC, Rodrigues CR, Loureiro NI, Castro HC et al. Design, synthesis, SAR, and biological evaluation of new 4-(phenylamino)thieno[2,3-b]pyridine derivatives. *Bioorganic & Medicinal Chemistry* 2006; 14: 5765-5770.



24. Vrabel M, Hocek M, Havran L, Fojta M, Votruba I et al. Purines bearing phenanthroline or bipyridine ligands and their RuII complexes in position 8 as model compounds for electrochemical DNA labeling – Synthesis, crystal structure, electrochemistry, quantum chemical calculations, cytostatic and antiviral activity. *European Journal of Inorganic Chemistry* 2007; 12: 1752-1769.
25. Paronikyan EG, Noravyan AS, Dzhagatspanyan IA, Nazaryan IM, Paronikyan RG. Synthesis and anticonvulsant activity of isothiazolo [5,4-b] pyrano (thiopyrano) [4,3-d]pyridine and isothiazolo [4,5-b]-2,7-naphthyridine Derivatives. *Pharmaceutical Chemistry Journal* 2002; 36: 465-467.
26. Firke SD, Firake BM, Chaudhari RY, Patil VR. Synthetic and pharmacological evaluation of some pyridine containing thiazolidinones. *Asian Journal of Research in Chemistry* 2009; 2: 157-161.
27. Pan P, Xie S, Zhou Y, Hu J, Luo H et al. Dual functional cholinesterase and PDE4D inhibitors for the treatment of Alzheimer's disease: Design, synthesis and evaluation of tacrine-pyrazolo[3,4-b]pyridine hybrids. *Bioorganic & Medicinal Chemistry Letters* 2019; 29: 2150-2152.
28. Radwan MAA, Alshubramy MA, Abdel-Motaal M, Hemdan BA, El-Kady DS. Synthesis, molecular docking and antimicrobial activity of new fused pyrimidine and pyridine derivatives. *Bioorganic Chemistry* 2020; 96: 103516.
29. Ekiz M, Tutar A, Ökten S, Bütün B, Koçyiğit ÜM et al. Synthesis, characterization, and SAR of arylated indenoquinoline-based cholinesterase and carbonic anhydrase inhibitors. *Arch Pharm Chemistry Life in Science* 2018; 351: e1800167.
30. Barut EN, Barut B, Engin S, Yıldırım S, Yaşar A et al. Antioxidant capacity, anti-acetylcholinesterase activity and inhibitory effect on lipid peroxidation in mice brain homogenate of *Achillea millefolium*. *Turkish Journal of Biochemistry* 2017; 42: 493-502.
31. Barut B, Barut EN, Engin S, Özel A, Sezen FS. Investigation of the antioxidant,  $\alpha$ -glucosidase inhibitory, anti-inflammatory, and DNA protective properties of *Vaccinium arctostaphylos* L. *Turkish Journal of Pharmaceutical Sciences* 2019; 16: 175-183.
32. Biyiklioglu Z, Barut B, Özel A. Synthesis, DNA/BSA binding and DNA photocleavage properties of water soluble BODIPY dyes. *Dyes and Pigments* 2018; 148: 417-428.

## SUPPLEMENTARY INFORMATION

### 1. Materials and equipment

4-Hydroxybenzaldehyde, 3-(3-chloropropyl)pyridine, 2,4-dimethylpyrrole were purchased from commercial suppliers. All reagents and solvents were of reagent grade quality and were obtained from commercial suppliers. The IR spectra were recorded on a Perkin Elmer 1600 FT-IR Spectrophotometer, using KBr pellets.  $^1\text{H}$  and  $^{13}\text{C}$ -NMR spectra were recorded on a Bruker Avance III 400 MHz spectrometers in DMSO- $d_6$ , and chemical shifts were reported ( $\delta$ ) relative to  $\text{Me}_4\text{Si}$  as internal standard. MALDI-MS of complexes were obtained in dihydroxybenzoic acid as MALDI matrix using nitrogen laser accumulating 50 laser shots using Bruker Microflex LT MALDI-TOF mass spectrometer (Bremen, Germany). Optical spectra in the UV-vis region were recorded with a Perkin Elmer Lambda 25 spectrophotometer. The inhibitory properties of the enzymes were carried out using Thermo Scientific Multiskan<sup>TM</sup> Go Microplate Spectrophotometer using a 96-well microplate reader. Electrophoresis was performed using BioRad, Wide Mini-Sub Cell GT Cell.

### 2. Biological effects

#### 2.1. AChE and BuChE inhibitory assay

AChE and BuChE inhibition of the compounds were measured according to Ingkaninan's method with some modifications using a 96-well microplate reader [1]. Galantamine was used as a positive control and DMSO (final concentration 1%) as blank. Tris-HCl buffer pH 8 (50  $\mu\text{L}$ , 50 mM), DTNB (125  $\mu\text{L}$ , 3 mM), AChE/BuChE (25  $\mu\text{L}$ , 0.2 U/mL) and the compounds were added in the microplate and incubated for 15 min at

room temperature. Afterwards, 25  $\mu$ L of 15 mM the substrate (AChI/BChI) was added to start enzymatic reaction. The absorbance was measured at 412 nm using microplate reader. AChE and BuChE inhibition percentage of the compounds was calculated using the formula 1. Formula 1= % Inhibition:  $(A-B)/A \times 100$ . A is the activity of the enzyme without compound, and B is the activity of the enzyme with compound. The inhibitory effect of the compounds was expressed as the concentration, which inhibited 50% of the enzyme activity ( $IC_{50}$ ).

Lineweaver–Burk and Dixon plots were performed to determine inhibitory type, and constant ( $K_i$ ) values of BDPY-4 was the most potent compound on AChE [2,3]. The kinetic analysis was conducted by various substrate concentrations (5, 10, 15, and 20 mM) in the absence and presence of BDPY-4.

AChE binding studies of BDPY-4 were carried out using UV-Vis spectroscopy to investigate the interaction of compound with protein. A stock solution of AChE was prepared in the buffer and stored at 4 °C for further use. In this work, a fixed concentration of AChE was taken (10  $\mu$ M), and various concentrations of BDPY-4 (0-20  $\mu$ M) were added to AChE solution [4].

## **2.2. $\alpha$ -Glucosidase inhibitory assay**

$\alpha$ -Glucosidase inhibition assay was performed as previously reported with some modifications [5]. Acarbose was used as a positive control, and DMSO (final concentration 1) as blank. The compounds (50  $\mu$ L) in phosphate buffer pH 6.9,  $\alpha$ -glucosidase (100  $\mu$ L, 0.5 U/mL) were added and allowed to react for 20 min in a microplate. After incubation, 4-pNPG (50  $\mu$ L, 5 mM) was added and incubated for 20 min at room temperature. The absorbance was measured at 405 nm using a 96-well

microplate reader.  $\alpha$ -glucosidase inhibition percentage of the compounds was calculated using the formula 1.

### **2.3. Supercoiled pBR322 plasmid DNA cleavage experiments**

Supercoiled pBR322 plasmid DNA nuclease effects of the compounds were investigated using agarose gel electrophoresis. DMSO (final concentration 1%) was used as a negative control. Supercoiled pBR322 plasmid DNA was treated with increasing concentrations of the compounds (50 and 100  $\mu$ M) in the buffer containing 50 mM Tris-HCl pH 7.0. All samples were incubated at 37 °C for 30 min and 60 min. Afterwards, loading buffer (bromophenol blue, xylene cyanol, glycerol, ethylenediaminetetraacetic acid, sodium dodecyl sulfate) was added, and the samples were loaded on agarose gel (0.8%) with ethidium bromide staining in TAE buffer (Tris-acetic acid-EDTA). Electrophoresis was performed at 100 V for 90 min [6].

### **References**

1. Barut EN, Barut B, Engin S, Yıldırım S, Yaşar A et al. Antioxidant capacity, anti-acetylcholinesterase activity and inhibitory effect on lipid peroxidation in mice brain homogenate of *Achillea millefolium*. Turkish Journal of Biochemistry 2017; 42: 493-502.
2. Lineweaver H, Burk D. The determination of enzyme dissociation constant. Journal of American Chemical Society 1934; 56: 658–661.
3. Butterworth P. The use of Dixon plots to study enzyme inhibition. Biochimica et Biophysica Acta (BBA) – Enzymology 1972; 289: 251-253.

4. Wang S, Wu C, Liu Z, You H. Studies on the interaction of BDE-47 and BDE-209 with acetylcholinesterase (AChE) based on neurotoxicity through fluorescence, UV-Vis spectra, and molecular docking. *Toxicology Letters* 2018; 287: 42-48.
5. Şöhretoğlu D, Sari S, Özel A, Barut B,  $\alpha$ -Glucosidase inhibitory effect of *Potentilla astracanica* and someisoflavones: Inhibition kinetics and mechanistic insights throughin vitro and in silico studies. *International Journal of Biological Macromolecules* 2017; 105: 1062-1070.
6. Barut B, Yalçın CÖ, Sari S, Çoban Ö, Keleş T et al. Novel water soluble BODIPY compounds: Synthesis, photochemical, DNA interaction, topoisomerases inhibition and photodynamic activity properties. *European Journal of Medicinal Chemistry* 2019; 183: 111685.

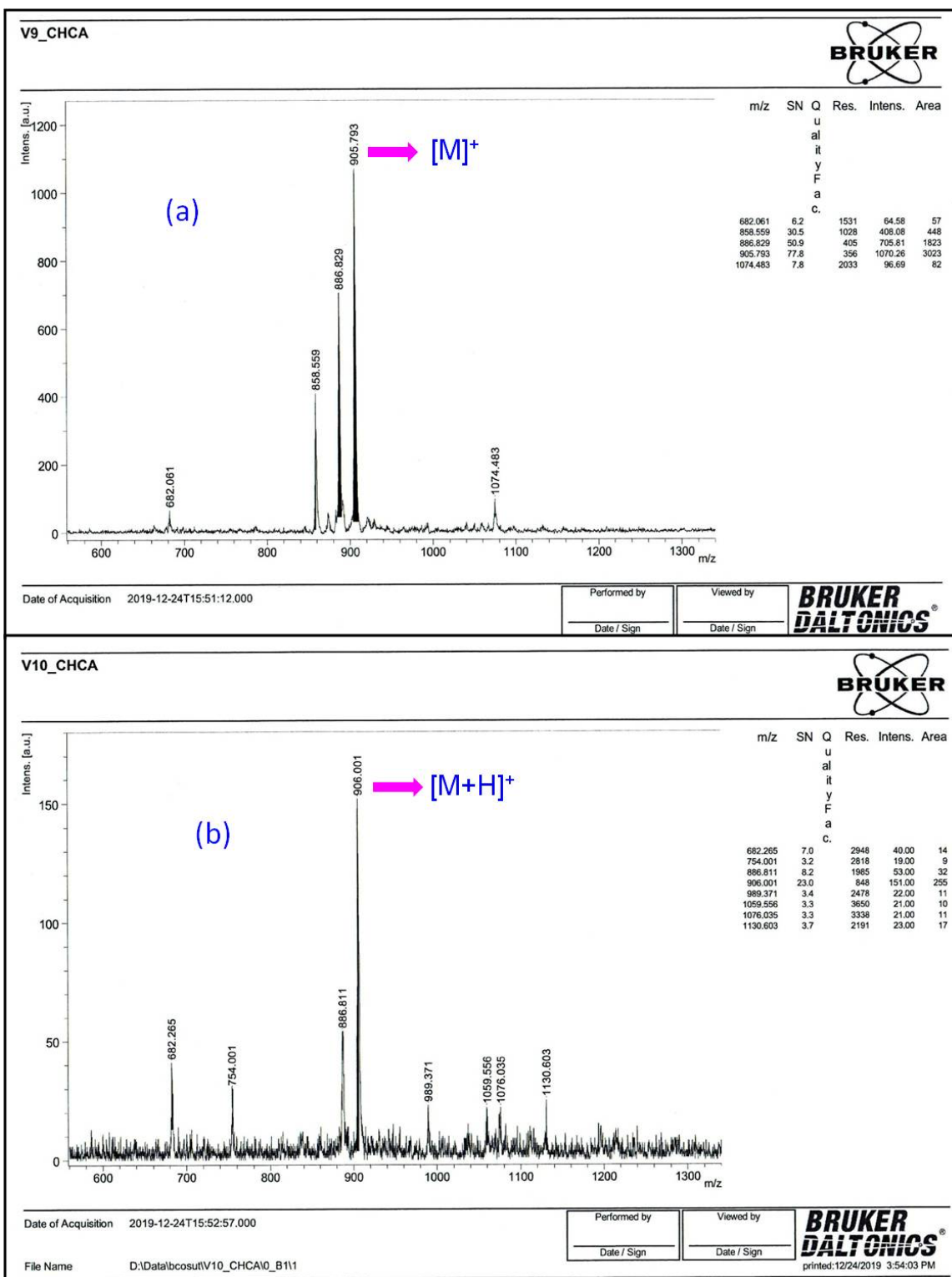


Figure S1. (a) MALDI-TOF MS spectrum of **BDPY-4**. (b) MALDI-TOF MS spectrum of **BDPY-5**.